JPET Fast Forward. Published on January 21, 2003 as DOI:10.1124/jpet.102.044024

Moment Analysis of Metabolic Heterogeneity: Conjugation of Benzoate with Glycine in Rat Liver Studied by Multiple Indicator Dilution Technique

Andreas J. Schwab[1], Lei Tao[2], Manjinder Kang[2], Lingjie Meng[2], and K. Sandy Pang[2,3,4]

[1]McGill University Medical Clinic, McGill University Health Centre, Montreal, Canada H3G 1A4 (AJS)

[2]Departments of Pharmaceutical Sciences (LT, MK, LM, and KSP) and [3]Pharmacology (KSP), Faculties of Pharmacy and Medicine, University of Toronto, Toronto, Canada M5S 2S2

[4]To whom correspondence should be addressed.

Running head: Moment analysis of metabolic heterogeneity

Address for proofs:
Dr. K. S. Pang
Faculty of Pharmacy
University of Toronto
19 Russell Street
Toronto, Ontario
Canada M5S 2S2

Phone: (416) 978-6164
FAX: (416) 978-8511
e-mail: ks.pang@utoronto.ca

Abstract:	249	words
Introduction:	742	words
Discussion:	1380	words
Tables:	5	
Figures:	7	
References:	37	

Abbreviations: AUC, area under the curve of benzoate; AUC_M, area under the curve formed metabolite; AUC_{PM}, area under the curve of the preformed metabolite; BA, benzoic acid; HA, hippuric acid; MID, multiple indicator dilution technique; PP, periportal; PV, perivenous; MTT, mean transit time of benzoate; MTT_M, mean transit time of the formed metabolite; MTT_{PM}, mean transit time of the preformed metabolite; TLC, thin layer chromatography

Abstract

Metabolic zonation was assessed with the multiple indicator dilution (MID) technique in the single pass perfused rat liver with use of moment analysis of the formed metabolite (M) data. During single-pass, retrograde rat liver perfusion with 17 μM benzoate, a bolus containing tracer preformed metabolite [^{3}H]hippurate (PM) was injected rapidly into the hepatic vein at 20 min post-perfusion, followed by injection of a second bolus containing [^{14}C]benzoate at 30 min. Both doses also contained noneliminated reference indicators (^{51}Cr-labeled red blood cells, ^{125}I-labeled albumin, [^{14}C]- or [^{3}H]sucrose, and D_2O). The steady-state extraction ratio of benzoate, the area under the curve (AUC) and its mean transit time (MTT) during retrograde flow were identical to those previously observed for prograde flow. Values of AUC_{PM} and MTT_{PM} and AUC_{M} were also similar to previously published prograde data, but the MTT_{M} with retrograde perfusion was smaller than that for prograde perfusion. This, according to theory based on the tubes-in-series model, was consistent with perivenous enrichment of glycination activity when transport of drug was even and when the ratio of drug influx/efflux coefficient exceeded that for metabolite. Similar benzoate transport in periportal, homogeneous and perivenous isolated rat hepatocytes existed, and the influx/efflux coefficients (partition ratio) of benzoate from MID indeed exceeded that of hippurate. However, metabolism by zonal hepatocytes failed to reveal the anticipated metabolic zonation, and this is due likely to the shallow gradient of metabolic activity. The study demonstrates that moment theory is useful in delineating the perivenous enrichment of glycine conjugation activity.

Introduction

Drug removal by the liver involves the microcirculation, binding-debinding, transport, metabolism, and excretion, and is a distributed-in-space phenomenon that is modulated by zonation. A common method for probing enzyme zonation in absence of a transport barrier is single-pass prograde/retrograde perfusion of the rat liver preparation (Pang and Terrell, 1981; St-Pierre et al., 1989). With prograde perfusion, perfusate enters the portal vein and exits at the hepatic vein, first recruiting upstream then downstream enzymes. With retrograde perfusion, flow enters the hepatic vein and exits the portal vein such that zonal distributions of enzymes appear reversed (Pang and Terrell, 1981; Pang et al., 1983). A more elaborate perfusion protocol is the dual perfusion of the hepatic artery (HA) and portal vein, or the hepatic vein (HV). If the substrate is delivered via HA single-pass to the liver with blank perfusate flowing retrogradely (HAHV), substrate will be confined to the periportal (PP) space. Conversely, with prograde flow of blank perfusate entering the portal vein (HAPV), substrate delivered from HA is swept across the entire liver (Pang et al., 1988). The removal rate constants for the respective regions may be obtained upon normalization of the metabolic activity to the cellular water spaces accessed (Chiba et al., 1994).

By contrast, assessment of metabolic heterogeneity behind a transport barrier in the intact liver is more complex. The metabolic rates will depend on the transport of the drug and metabolite and whether the enzyme distribution is periportal (PP) or perivenous (PV). It is known that if transport across the hepatocyte membrane is poor, the fate of formed and preformed metabolites may differ (Sato et al., 1986; deLannoy and Pang, 1987; Schwab and Pang, 1999). Although there exist a few reports on the use of metabolite data to assess enzyme zonation after pulse injection of drug to the perfused rat liver preparation (Mellick et al., 1994; Ballinger et al., 1995), the basis for estimation has not been rigorously developed theoretically. A recent theoretical treatise had examined the influence of enzyme zonation on the AUC and MTT of drugs and metabolites and the transmembrane transport when the liver is

viewed as two half-parallel tubes arranged in series, or the tubes-in-series model (Schwab and Pang, 1999). Not unexpectedly, the mean residence time of the formed metabolite (MTT_M) depended on both transporter activities and localization of enzymes.

In this communication, we hypothesized that moment analysis of the metabolite is useful for examination of enzyme heterogeneity. Benzoate metabolism by glycine conjugation was chosen to illustrate the principle. A perivenous (zone 3) predominance of glycine conjugation has been inferred from HAPV and HAHV liver perfusion studies (Chiba et al., 1994). The metabolite, hippurate, undergoes saturable, barrier-limited transport into the rat liver, and is neither metabolized nor excreted into bile (Yoshimura et al., 1998). Benzoate also undergoes barrier-limited transport, but is transported linearly and rapidly into hepatocytes at concentrations below 1 mM (Schwab et al., 2001). Transport is likely attributed to the monocarboxylic acid transporter MCT1 (Tamai et al., 1999) that transports *L*-lactate and is evenly distributed in the acinus (Staricoff et al., 1995). Although the mitochondria space for metabolism constitutes an added, intracellular compartment (Chiba et al., 1994; Schwab et al., 2001), the attributes are ideal for the testing of the principles of moment analysis on enzyme zonation. In this study, a bolus containing tracer preformed [^{3}H]hippurate (PM) was injected rapidly into the hepatic vein of the rat liver at 20 min post-perfusion to characterize the hippurate transfer coefficients. This was followed by a second injection containing [^{14}C]benzoate at 30 min to characterize the transfer and metabolic coefficients of benzoate. Both injected doses also contained noneliminated reference indicators (^{51}Cr-labeled red blood cells, ^{125}I-labeled albumin, [^{14}C]- or [^{3}H]sucrose, and D_2O). The derived retrograde outflow data (17±1 μM benzoate) were analyzed according to the barrier-limited, variable transit time model of Goresky and were compared to those observed previously for prograde flow under first-order conditions (< 200 μM benzoate) (Schwab et al., 2001). However, due to our inability to encompass heterogeneity into the Goresky model, the previously developed tubes-in-series model was extended to encompass heterogeneity in mitochondrial metabolism behind transport barriers (Schwab and Pang, 1999). The expectations were the unchanged area under

the curve for preformed (PM) and formed (M) hippurate, an unchanged MTT_{PM} for PM but a smaller MTT_{M} for formed hippurate for retrograde flow since metabolic activity is distributed in the perivenous region. We further studied zonal transport and metabolism of benzoate with enriched, zonal rat hepatocytes.

Methods

Materials

Benzoic acid, hippuric acid and bovine serum albumin (fraction V) were obtained from Sigma Chemical Co. (St. Louis, MO). [^{14}C]Benzoic acid (specific activity, 110 mCi/mmol) and the [2-^{3}H]glycine (specific activity, 43.4 Ci/mmol) used for the synthesis of hippurate (Yoshimura et al., 1998) were obtained from American Radiolabeled Chemicals, Inc. (St Louis, MO) and DuPont Canada, Inc. (Markham, ON, Canada), respectively. [^{51}Cr]Sodium chromate (specific activity 5392 mBq/mg), [^{125}I]-labeled serum albumin (specific activity 0.46 mBq/mg) and $^{2}H_2O$ (> 99.98% pure) were procured from Merck Frosst, Montreal, QC, Canada. [^{14}C]Sucrose (4.95 mCi/mmol) and [^{3}H]sucrose (12.3 Ci/mmol) were purchased from NEN Life Science Products (Boston, MA). Digitonin was obtained from Fluka Chemie (Buchs, Switzerland). Collagenase was purchased from Boehringer Mannheim (Oakville, ON). All reagents used were of glass-distilled, high-performance liquid chromatographic grade, or the highest purity available (Fisher Scientific, Mississauga, ON, Canada).

Transport and Metabolic Studies in Isolated and Zonal Rat Hepatocytes

Isolation of homogeneous, periportal (PP), and perivenous (PV) rat hepatocytes. Enriched PP and PV hepatocytes and homogeneous hepatocytes from male, Sprague-Dawley rats (304 ± 28g, Charles River Canada, St. Constant, QC, Canada) were prepared according to the digitonin/collagenase perfusion method of Lindros and Pentïlla (1985), with modifications (Tan et al., 1999). The rats were housed in accordance with approved protocols of the University of Toronto Animal Committee, kept under artificial light on a 12:12 h light-dark cycle and allowed free access to water and food *ad libitum.* Hepatocyte viability was assessed by Trypan blue exclusion and averaged 93 ± 1.4% for the transport studies and 94 ± 2.8% for the metabolism studies. Zonal enrichment was defined with respect to the activities of alanine aminotransferase (ALT) and glutamine synthetase (GS), assayed by a commercially available kit (Sigma) and by a standard UV method (Tan et al., 1999; Tirona et al., 1999), respectively;

the PP:PV ratio was 1.5 for ALT and 12 for GS. Protein was assayed by the method of Lowry et al (1951).

Uptake of benzoate by isolated and zonal rat hepatocytes. Uptake studies were conducted as outlined previously (Tirona et al., 1999). All buffers were pre-gassed with Carbogen (95% O_2, 5% CO_2 v/v, Canox Gas, Mississauga, ON). After pre-incubation in an atmosphere of Carbogen for 10 min at 37°C, uptake of [^{14}C]benzoate (and 1 and 400 μM with 215,000 ± 102,000 dpm/ml) and [^{3}H]sucrose (383,000 ± 301,000 dpm/ml), an interstitial space marker, by PP (n = 3) and PV hepatocytes (n = 3) and isolated (homogeneous) hepatocytes (n = 4) was examined over the course of 1 min in 1.67 x 10^6 cells. Samples were removed at 15, 30, 45, and 60 sec for rapid centrifugation through a layer of silicon oil (100 μl of density 1.02 g/ml) into the lowest layer of 50 μl of 3N NaOH. After removal of the tips into a 20-ml glass scintillation vial and left overnight, 50 μl of 3 N H_2SO_4 was added to neutralize the sample. After the addition of scintillation fluor (Ready Safe, Beckman Coulter, Canada, Mississauga, Canada), the radioactivity of the cell and the supernatant (25 μl) were quantified in a liquid scintillation spectrometer (LS5801, Beckman Canada, Mississauga, ON, Canada). The extracellular volume entrapped in the cellular compartment was found by the [^{3}H]sucrose content, and a correction was made in the determination of cellular contents on [^{14}C]benzoate uptake.

Metabolism of benzoate in zonal rat hepatocytes. Cell suspensions of PP or PV hepatocytes, preincubated at 37°C for 10 min, were added to mixtures of [^{14}C]benzoate and unlabeled benzoate to result in concentrations of 480,000 ± 136,000 dpm/ml and 1 μM in 1.6 to 1.7 x 10^6 cells/ml. Duplicate samples (100 μl) were retrieved simultaneously at various times (0.5 to 7.5 min) directly into a 1.5 ml microcentrifuge tube containing 0.5 ml acetonitrile (and internal standard, methoxybenzoic acid) for HPLC analysis using a reverse-phase Beckman Ultrasphere column as previously described (Chiba et al., 1994; Schwab et al., 2001; Cong et al., 2001). The samples were mixed well and stored at –20°C until analysis. After thawing and centrifugation, 200 μl of the sample was injected directly onto the HPLC. Standards of known,

different counts were processed in an identical fashion for construction of the calibration curve.

Rat Liver Perfusion

Male Sprague-Dawley rats (n = 8; 296 ± 9 g; livers were 11 ± 2.2 g) served as liver donors. *In-situ* single pass liver perfusion under retrograde flow was carried out as previously described (St-Pierre et al., 1989) with perfusate (12 ml/min) at 37°C entering *via* the hepatic vein and exiting *via* the portal vein; the hepatic artery was ligated. Perfusate consisted of bovine erythrocytes (20%), freshly obtained and washed (kind gift of Ryding-Regency Meat Packers, Toronto, ON, Canada), 5% bovine serum albumin and 17 mM glucose (Travenol Labs, Deerpark, IL) in Krebs-Henseleit bicarbonate solution (pH 7.4). Perfusate was gassed simultaneously with 95% oxygen-5% carbon dioxide (Matheson, Mississauga, ON) and oxygen (BOC Gases, Whitby, ON), and the pH, monitored by an "on-line" flow-through pH electrode (Orion, Boston, MA), was maintained at 7.4 by adjusting the proportion of the two gas supplies. Three to five inflow and outflow perfusate samples, collected during steady state, were used for determination of the average input (C_{In}) and output (C_{Out}) perfusate concentrations of unlabeled benzoate and hippurate; both benzoate and hippurate do not distribute into red blood cells (Yoshimura et al., 1998; Schwab et al., 2001). Bile samples were collected for the first 15 min and at 5 to 10 min intervals thereafter up to 60 min to monitor the excreted radioactivity and the bile flow; the total recovery relative to the injected dose was found to be minimal.

Multiple Indicator Dilution. Two consecutive injections (0.23 ml) were made within each liver perfusion study with retrograde flow at 20 and 30 min, respectively, after the initiation of perfusion, as described previously (Goresky, 1963; Schwab et al., 2001). The first injection mixture contained ^{51}Cr-labeled erythrocytes (0.34 ± 0.034 μCi), ^{125}I-labeled albumin (2.3 ± 0.16 μCi), [^{14}C]sucrose (0.34 ± 0.09 μCi), $^{2}H_2O$ (0.09 ± 0.0056 ml) and [^{3}H]hippurate (1.36 ± 0.16 μCi) to define the transport parameters pertaining to the preformed metabolite. The second mixture contained ^{51}Cr-labeled erythrocytes (0.28 ± 0.023 μCi), ^{125}I-labeled

albumin (2.3 ± 0.26 μCi), [^{3}H]sucrose (0.30 ± 0.1 μCi), and [^{14}C]benzoate (1.14 ± 0.21 μCi). Each injected mixture contained a constant concentration of unlabeled benzoate (17 ± 1.3 μM) in a composition otherwise identical to that of the perfusate, and was introduced into the inflow system by an electronically controlled injection valve, and subsequent outflow samples were continuously being collected for a total of 180 sec and 280 sec, respectively, for the first and second injections, as described previously (Schwab et al., 2001). The hematocrits of the injection mixture and the perfusate were determined for each experiment by use of a hematocrit centrifuge (Model MB Microhematocrit Centrifuge, IEC, Fisher Scientific). Sham experiments (without liver) were conducted to characterize the dispersion due to the injection device and the inflow and outflow catheters and for estimation of the mean transit time of the catheters.

Quantitation of Radioisotopes in MID Study And Assay of Unlabeled Benzoate and Hippurate in Perfusate and Bile

The ^{51}Cr and ^{125}I radioactivities in outflow blood perfusate samples and the injected dose were assayed by gamma counting (Cobra II, Canberra-Packard Canada, Mississauga, ON, Canada). Perfusate plasma was separated from red blood cells by centrifugation, and the contained [^{3}H]- and [^{14}C]- radioactivities in outflow perfusate plasma (25 to 200 μl) and the plasma dose (1:10 dilution, 25 μl) were made up to 200 μl with blank perfusate plasma. After the addition of 800 μl acetonitrile for deproteinization, 800 μl of the supernatant was removed for liquid scintillation counting (LS5801, Beckman Canada, Mississauga, ON, Canada). $^{2}H_2O$ in perfusate plasma was assayed by Fourier transform infrared spectrometry as previously described (Pang et al., 1991). The perfusate plasma sample (100 or 200 μl) from the second injection was added acetone (4:1 v/v) for deproteinization, and the supernatant fraction containing the [^{14}C]Benzoate and [^{14}C]hippurate was removed and spotted onto the origin of the Silica Gel GF TLC plate (250 μm, Analtech, Newark, DE) that was prespotted with unlabeled benzoate and hippurate. The outflow perfusate and bile samples were developed in a solvent system of chloroform : cyclohexane : acetic acid (80:20:10, v/v/v), as described

previously (Schwab et al., 2001). The scraped fractions after TLC development were added 0.5 ml water, mixed and subjected to liquid scintillation counting as described earlier (Schwab et al., 2001).

The concentrations of unlabeled benzoate and hippurate in perfusate plasma samples and bile were assayed by high performance liquid chromatography, as previously described (Chiba et al., 1994; Schwab et al., 2001). Perfusate plasma (500 µl) was added the internal standard, methoxybenzoic acid (50 µl of 16 µg/ml solution in water) and was deproteinized with 800 µl of acetonitrile, dried under nitrogen, and reconstituted for injection into the HPLC. A solvent gradient, consisting of 0.5% acetic acid and acetonitrile was utilized. Standards for calibration curves (varying amounts of unlabeled benzoate) were processed under identical conditions.

Theory

The theory pertaining to fits to the hippurate and benzoate outflow data according to the Goresky model is based on homogeneous enzyme and transporter functions but heterogeneous flow behavior (Fig. 1). The equations that have been described in detail for prograde flow are presently utilized but will not be repeated here (Schwab et al., 2001). The fit to the Goresky model will provide the transport parameters for hippurate (first dose) and benzoate (second dose) as well as the mitochondrial transfer and metabolic rate constants. However, we have not yet found a consistent way to model enzyme zonation in the Goresky-type model. Hence, we had adopted an alternate approach for the detection of enzyme zonation from prograde and retrograde MID data by extending the existing theory on the tubes-in-series model (Schwab and Pang, 1999, Fig. 1A). With the present precursor-product pair, benzoate and hippurate, however, glycine conjugation occurs within the mitochondria (Gatley and Sherratt, 1977), evoking consideration of an extra pool (Fig. 1B). Results of MID studies by Schwab et al. (2001) indeed confirmed the involvement of a deep compartment for metabolism. Hence, the theory was extended to reflect this (see Appendix 1). Moments may then be calculated for this model and the results are summarized in Table 1.

Enzyme Zonation Within the Tubes-in-Series Model. The rate constant for metabolic transformation is again treated as a function of the relative position within the acinus, denoted by τ (where $\tau = 0$ represents a position adjacent to the portal venule, and $\tau = 1$ represents one adjacent to the central venule) to represent enzyme zonation. Conversely, rate constants for transmembrane transport (k_{13}, k_{31}, k_{25}, k_{52}, k_{34}, and k_{43}) are treated as constants to represent homogeneously distributed transporter activity. This assumption is validated, at least for (k_{13}) in the zonal-hepatocyte uptake study of benzoate. For the formulation of Laplace transforms and moments of outflow profiles, the sinusoid was considered as two half sinusoids arranged in series, each with a transit time of $0.5\,MTT_{ref}$. A stepwise change of k_{45} at $\tau = 0.5$ was assumed such that

$$k_{45}(\tau) = (1 + r)\,\bar{k}_{45},\ 0 < \tau < 0.5\ \mathrm{MTT}_{ref} \quad (1)$$

$$k_{45}(\tau) = (1 - r)\,\bar{k}_{45},\ 0.5\ \mathrm{MTT}_{ref} < \tau < \mathrm{MTT}_{ref} \quad (2)$$

where $\bar{k}_{45}$ is the length-averaged value of $k_{45}(\tau)$, the metabolic rate constant, and r is a heterogeneity parameter with values between –1 and 1. As defined previously, positive values of r denote a predominantly periportal enzymic distribution and negative values of r denote predominantly a perivenous enzymic distribution (Schwab and Pang, 1999). Special cases include exclusively periportal (PP) enzyme distribution ($r = 1$) and exclusively perivenous (PV) enzyme distribution ($r = –1$); for $r = 0$, the enzyme distribution is even or uniform. Various values of r ranging from –1 to +1 were used to explore the impact of intermediate enzyme zonation on the moments of drugs and metabolites. As shown previously, the overall unit impulse response of subsystems connected in series is given as the convolution of the individual unit impulse responses (Lassen and Perl, 1979; Bronikowski et al., 1987; Schwab et al., 2001). Laplace transforms and AUC's are obtained as the products of those of the outflow profiles of the subsystems, whereas MTT's are their sums.

For the PP case ($r = 1$), the outflow profile of the metabolite is the convolution of the outflow profile of the metabolite formed from the parent drug from an upstream partial sinusoid or first half-tube (where k_{45} is twice the length-averaged value) and the outflow profile of an existing (preformed) metabolite for a downstream partial sinusoid or second half-tube. For the PV case ($r = –1$), the overall outflow profile of the metabolite is the convolution of the outflow profile of the parent drug from an upstream partial sinusoid where no conversion takes place (k_{45} is set to zero), and the outflow profile of the metabolite formed from the parent drug from a downstream partial sinusoid (where k_{45} is set to twice the length-averaged value). With stepwise increasing or decreasing enzyme activity, the moments for the metabolite outflow curves are evaluated as follows,

JPET Fast Forward. Published on January 21, 2003 as DOI: 10.1124/jpet.102.044024
This article has not been copyedited and formatted. The final version may differ from this version.

$$AUC_M = AUC_{M,PP}\ AUC_{PM,PV} + AUC_{PP}\ AUC_{M,PV} \quad (3)$$

$$MTT_M = \frac{(MTT_{M,PP} + MTT_{PM,PV})AUC_{M,pp}AUC_{PM,pv}}{AUC_{M,PP}AUC_{PM,PV} + AUC_{PP}AUC_{M,PV}} + \frac{(MTT_{PP} + MTT_{M,PV})AUC_{PP}AUC_{M,PV}}{AUC_{M,PP}AUC_{PM,PV} + AUC_{PP}AUC_{M,PV}} \quad (4)$$

where AUC_{PP}, $AUC_{M,PP}$, and $AUC_{PM,PP}$ are expressions for the AUC of the parent drug, the formed metabolite (subscript M), and the preformed metabolite (subscript PM), respectively, for the periportal part of the acinus, and AUC_{PV}, $AUC_{M,PV}$, and $AUC_{PM,PV}$ are the corresponding values for the perivenous part. The mean transit times MTT_{PP}, $MTT_{M,PP}$, $MTT_{M,PV}$, and $MTT_{PM,PV}$ are defined equivalently. The algebraic expressions (see Appendix) were derived using MathView software (Waterloo Maple Inc., Waterloo, ON, Canada) on a Power Macintosh computer.

Data Treatment

For the multiple indicator dilution data, the concentrations of radiolabels in the outflow perfusate were normalized to the respective doses, yielding fractional recoveries (or concentration/dose). The fractional recovery-integral (or area under the curve, AUC) and area under the moment curve (AUMC or the integral of the product of fractional recovery and time at mid-intervals) of the outflow data of benzoate and hippurate were estimated by the spline function of IMSL (Visual Numerics, Houston, TX). The ratio of AUMC/AUC furnished the mean transit time, MTT. Tracer recoveries were obtained by multiplying AUCs with perfusate flow and were virtually complete for the noneliminated reference indicators and the [^{3}H]hippurate and [^{14}C]benzoate doses; the latter recovery was assessed as the summed recoveries for ([^{14}C]benzoate and [^{14}C]hippurate.

Modeling of hepatic hippurate and benzoate disposition. The outflow profiles of the non-metabolized indicators, ^{51}Cr-labeled erythrocytes, ^{125}I-labeled albumin, [^{3}H]- or [^{14}C]sucrose, and ^2H_2O, were evaluated by linear superposition as described previously (St-Pierre et al.,

1989; Xu et al., 1990; Schwab et al., 2001). The kinetic model for the transport and metabolism of benzoate in the perfused rat liver has previously been validated (Schwab et al., 2001). In the absence of an established whole-organ model that includes enzyme zonation, the data were fitted to the homogeneous-enzyme model of Goresky, as done previously for the prograde experiments (Schwab et al., 2001). The outflow profiles (impulse responses) were calculated using an algorithm based on an approximation of the reference indicator curves by exponential sums as previously described (Schwab, 1984; Schwab et al., 2001).

The fit of outflow data from the first MID injection of tracer hippurate according to the Goresky model yielded the transfer coefficients for hippurate transport, k_{25} and k_{52}, and the parameter $\gamma_{rel,H}$, derived from the ratio of interstitial to vascular distribution spaces of hippurate, γ_H. These values (k_{25} and k_{52} and γ_H) were assigned as the parameters for [^{14}C]hippurate transport and for the interstitial-vascular distribution space ratio of hippurate for the same liver. Fitting of the [^{14}C]benzoate and [^{14}C]hippurate profiles from the second MID injection furnished the transfer coefficients for benzoate transport, k_{13} and k_{31}, the exchange parameters between intracellular pools, k_{34} and k_{43}, the coefficient for metabolism, k_{45}, and the parameter $\gamma_{rel,B}$, derived from the ratio of the interstitial to the vascular distribution space of benzoate γ_B.

For analysis of outflow profiles, transport functions (impulse responses) of the liver were obtained by numerical deconvolution of experimental outflow profiles with the transport function of the combined injection and collection devices (the catheter transport function), using an algorithm obtained from the National Simulation Resource in Mass Transport and Exchange, University of Washington, Seattle, Washington. The theoretical outflow dilution profiles of non-eliminated reference indicators were obtained by convolution of calculated transport functions with the catheter transport function (Yoshimura et al., 1998), using an algorithm for numerical integration (QDAG from IMSL, Visual Numerics, Houston, TX). Convolution with the catheter transport function was incorporated into the algorithm for calculating the outflow profiles of benzoate and hippurate (Schwab et al., 2001).

Statistics

All data were presented as mean ± S.D. ANOVA was used to compare differences in the mean values. A *P* value of <.05 was viewed as significant.

Results

Uptake and Metabolism of Benzoate by Zonal Hepatocytes. The amounts of benzoate accumulated within hepatocytes, estimated as the radioactivity in cell pellets, were linear with time within one-min of sampling. The regression slopes yielded similar uptake rates for the PP, PV, and homogeneous isolated rat hepatocytes at the low BA (1 μM) and high (400 μM) concentrations tested (Fig. 2). The results paralleled those for the uptake of *L*-lactate, the model substrate of MCT2, in zonal rat hepatocytes (Staricoff et al., 1995). The disappearance of benzoate (1 μM) in the incubation mixture upon incubation was similar for both PP and PV hepatocytes (n = 4 preparations each). The rate of formation of hippurate was linear up to 5 min of incubation, and interpretation was based on data gathered up to 3 or 5 min (Fig. 3). No difference was found for hippurate formation from PP (5.86 ± 1.88 % initial concentration/min) and PV (5.25 ± 1.46 % initial concentration/min, $P > 0.05$) hepatocytes, nor for the decay rate constants of BA (0.0676 ± 0.0220 min^{-1} for PP cells and 0.0563 ± 0.0162 min^{-1} for PV cells) in the incubation system ($P > 0.05$).

AUC and MTT For the Tubes-in-Series Model. The solutions for AUC and MTT were shown in eqs. 3 and 4. For a drug such as benzoate that entails metabolism within a sequestered pool (see Fig. 1B), the apparent tissue to plasma partitioning of drug was given by $(k_{13}/k_{31})(1 + k_{34}/k_{43})$ due to the additional mitochondrial pool, whereas that for the preformed metabolite was given by k_{25}/k_{52}, and the ratio of these values yield the relative permeability characteristics of the drug and metabolite (Table 1). The area under the curve of the formed metabolite, AUC_M, was found to be constant for prograde and retrograde flow directions regardless of whether $(k_{13}/k_{31})(1 + k_{34}/k_{43}) > k_{25}/k_{52}$ or $(k_{13}/k_{31})(1 + k_{34}/k_{43}) < k_{25}/k_{52}$. By contrast, the MTT_M would change according to the values of $(k_{13}/k_{31})(1 + k_{34}/k_{43})$ vs. k_{25}/k_{52} and the flow direction (Table 1). These relationships were similar to those found in an earlier treatise when the tubes-in-series model was first developed in absence of the mitochrondrial compartment (Schwab and Pang, 1999).

Moment Analysis of Hippurate and Benzoate in MID Studies. The steady-state extraction ratio of benzoate (0.6) for retrograde flow (Table 2) was similar to that observed previously for prograde flow (data of Schwab et al., 2001). Representative outflow profiles of tracer [^{3}H]hippurate (first injection), of tracer [^{14}C]benzoate and its metabolite, [^{14}C]hippurate (second injection) and of the noneliminated indicators are shown in Figs. 4 and 5, respectively, for 17 μM benzoate in the inflow perfusate. The outflow profiles of the noneliminated indicators (labeled erythrocytes, albumin, sucrose, and $^{2}H_2O$) for the first and the second injections in outflow (portal venous) perfusate were increasingly dispersed. The total recoveries of the ^{51}Cr-, ^{125}I-, ^{14}C-, and ^{3}H-radiolabels and of $^{2}H_2O$ in the venous outflow samples were virtually complete (Table 3). All of the injected [^{3}H]hippurate returned to the vasculature as [^{3}H]hippurate, and the [^{14}C]benzoate returned as unchanged [^{14}C]benzoate or [^{14}C]hippurate, suggesting that benzoate was metabolized exclusively to hippurate and that both benzoate and hippurate were not significantly excreted.

The mean transit times of the vascular noneliminated indicators differed slightly between the two injections made at 20 and 30 min for the present studies (Table 4). The data, when compared to previous prograde data of Schwab et al. (2001), revealed that the values for total water volumes (sum of both cellular and extracellular water spaces) were greater than unity (Table 4). The apparently high value is due to the distention of the vasculature during retrograde flow, as described by St-Pierre et al. (1989) and Xu et al. (1990). The MTTs for labeled red blood cells, albumin, and sucrose were all increased with retrograde flow, especially for data of the first injection, although changes in the second injection were attenuated. The reason for the difference between the first and second injections was unknown, but may be due to a greater compliance with the slightly longer perfusion time. Higher sinusoidal volumes and sucrose (for the first injection) and albumin (for the second injection) sucrose Disse spaces were observed for retrograde flow (Fig. 6).

There was no change in the mean transit times for benzoate (MTT) and the preformed hippurate (MTT_{PM}) (Table 4). Although values for MTT_{PM} were similar to that of labeled

sucrose, the shapes of the curves differed due to partial entry of hippurate into the rat liver (Fig. 4). The [^{3}H]hippurate profile crossed over then peaked lower and earlier than the labeled sucrose curve and exhibited a more delayed downslope. The mean transit time of formed hippurate (MTT_M) in the present study was greater than MTT_{PM} but was much lower than that of Schwab et al. (2001) for prograde flow ($P < 0.05$). The PP/PV ratio of MTT_M exceeded unity. Moreover, values of MTT_M (67 ± 7 sec) significantly exceeded ($P <. 0.05$) the summed MTTs for preformed HA and BA (52 ± 6 sec). The same trend was also observed upon re-examination of the prograde data of Schwab et al. (2001); MTT_M (114 ± 32 sec) was significantly greater ($P < 0.05$) than the sum of the MTTs for preformed HA and BA (56 ± 13 sec).

Model Fits to Outflow Profiles of [^{3}H]Hippurate According to Goresky's Model. The outflow profile of hippurate obtained after injection of [^{3}H]hippurate during retrograde flow (Fig. 4) was similar to that described for prograde flow (Schwab et al., 2001). The optimal interstitial to sinusoid distribution ratio γ_H (0.30 ± 0.43) obtained after consideration of binding of hippurate to albumin in perfusate fluid, was smaller than the value of 1.08 ± 0.33 reported by Schwab et al., (2001) due to distention of the vasculature. The transfer coefficients (k_{25} and k_{52}, Table 5) differed for the influx coefficient (k_{25}) but not for the permeability surface area or PS product (0.049 ± 0.036 ml sec^{-1} g^{-1}) for the influx of hippurate between perfusate and hepatocytes. The ratio of k_{25} and k_{52}, or the equilibrium, partitioning ratio was 0.26 ± 0.07 and differed from that (0.82 ± 0.17) for prograde flow (Schwab et al., 2001).

Model Fits to Outflow Profiles of [^{14}C]Benzoate According to Goresky's Model. The outflow profile of benzoate obtained after injection of [^{14}C]benzoate during retrograde flow (Fig. 5) was similar to that described for prograde flow (Schwab et al., 2001). The optimal interstitial to sinusoid distribution ratio $\gamma_{B,}$ (0.45 ± 0.04) obtained after consideration of binding of benzoate to albumin in perfusate fluid (Chiba et al., 1994) was significantly smaller than the value of 0.97 ± 0.46 reported by Schwab et al. (2001) due to distention of the vasculature. Two of the coefficients (k_{31} and k_{34}, Table 5) differed from those for prograde flow, and the

permeability surface area product of benzoate was slightly greater, with the metabolic coefficient being smaller than those for prograde flow (Table 5). The ratio of k_{13} and k_{31}, or the equilibrium partitioning ratio was 0.7 ± 0.20 and differed from that for (1.68 ± 0.75) prograde flow (Schwab et al., 2001). However for these fits, $k_{13}/k_{31} > k_{25}/k_{52}$ for both retrograde and prograde flows.

Simulations Based on Tubes-in-Series Theory. Simulations were made based on the analytical solutions for the MTT_M (eq. 4) for prograde and retrograde flows and the values of k_{13},, k_{31}, k_{34}, k_{43} and k_{45} for benzoate and of k_{25} and k_{52} in Table 5. The condition for simulation was identical to the experimentally obtained, fitted parameters that revealed that the partition ratio for benzoate (ratio of influx /efflux rate constants) k_{13}/k_{31} $(1 + k_{34}/k_{43})$ being greater than that for hippurate (k_{25}/k_{52}). The resulting PP:PV ratio of MTT_M was plotted against *r*, the heterogeneity parameter. The simulations (Fig. 7) predicted that the PP:PV ratio of MTT_M exceeds unity for negative values of *r* and was less than unity for positive values of *r* for the tubes-in-series Model. Both the simulation with the tubes-in-series model and the observed data suggest the perivenous abundance of benzoate glycine conjugation activity, as found by Chiba et al. (1994).

Discussion

Metabolite behavior is highly complex and may differ from the kinetic behavior of a preformed metabolite entering an organ. Although the same transport function and enzyme(s) are involved in metabolite removal, perceptive differences exist due to the presence of a transport barrier for metabolite, barring the PM from entering and preventing M from leaving (deLannoy and Pang, 1987). The kinetic behavior of the formed metabolite (M) is highly dependent on the model of hepatic drug clearance — whether the well-stirred model, the parallel tube model, or the dispersion model (St-Pierre et al., 1992, Pang 1995) applies, and depending whether the permeability of drugs and metabolite is high or poor.

According to the well-stirred model, the kinetics of M is independent of drug behavior, and the MTT_M is the sum of the MTTs for highly permeable drug and preformed metabolite (Chan et al., 1985; St-Pierre et al., 1992; Mellick et al., 1997). For both the parallel tube and dispersion models, however, the kinetic behavior of M is predicated on drug kinetic behavior (St-Pierre et al., 1992). The difference on metabolite formation between the dispersion model (dispersive flow and some mixing) and the parallel tube model (plug flow, non-dispersive and no mixing) for flow-limited substrates in absence of enzyme heterogeneity is, however, small, and a similar trend persists when enzyme heterogeneity is added (St-Pierre et al., 1992). For these reasons, lower values for MTT_M are predicted for the parallel-tube and dispersion models in comparison with the well-stirred model for highly permeable drugs and metabolites (Roberts et al., 1988; St-Pierre and Pang, 1993a; 1993b; St-Pierre et al., 1992; Mellick et al., 1997). When permeabilities of the drug and the metabolite are low, however, MTT_M will exceed the sum of the mean transit times of the drug and the preformed metabolite (Mellick et al., 1997), since poor permeability of the metabolite retards entry of preformed metabolite but extends the sojourn time of the metabolite formed in the organ. This is confirmed by calculations that show that barrier limitation of transport of the metabolite may increase MTT_M beyond the sum of the mean transit times of the drug and the preformed metabolite even when the transport of the precursor is not barrier-limited.

The presence of an additional precursor pool such as the mitochondrial space where conjugation of benzoic acid takes place (Fig. 1B) will extend the mean transit times of the drug and the formed metabolite but will not affect that of the preformed metabolite. However, the presence of the additional mitochondrial pool would not affect the trends of the expected changes on the AUC_M and MTT_M with enzyme zonation (Table 1). Our observation that MTT_M for formed hippurate greatly exceeded the sum of the MTTs of benzoate and preformed hippurate is only suggestive of the poor permeability of hippurate. This finding is in agreement with the present transfer constants for hippurate, as well as those found in previous MID experiments (Yoshimura et al., 1998; Schwab et al., 2001) showing that the influx clearance of hippurate ($P_{25}S$) was less than the perfusate flow rate.

Interpretation of the AUC and MTT data of the present study depends on verifying the viability of the preparation at the times of both injections during retrograde flow. In previous experiments with retrograde perfusion of rat livers under similar conditions, measured rates of bile flow or oxygen consumption were not different from values obtained with prograde perfusion (St-Pierre et al., 1989; Xu et al., 1990), and inflow venous pressures were unchanged (St-Pierre et al., 1989) or only increased minimally (Xu et al., 1990). The observed difference in the hematocrit (Table 2) should not impact on liver viability or processing of benzoate and hippurate since both are not bound to RBC. However, distention was a hallmark of retrograde perfusion (St-Pierre et al., 1989; Xu et al., 1990), and this was evident from the blebbing of the curve form (shifting of maximum concentration to a lower value and at later time) with retrograde flow. Of note, the MTT and the volumes of the vascular indicators were enlarged and cellular water space, estimated by difference, was reduced for retrograde flow when compared to prograde data (Fig. 5), as found previously (St-Pierre et al., 1989; Xu et al., 1990). However, vascular volume distention during the second injection was much less severe than that for the first injection, indicating an adaptation process. The AUC and MTT of preformed species (hippurate or “PM” and benzoate) remained unchanged with both perfusion directions (Tables 3 and 4), and this finding strongly suggests that parameters pertaining to the

formed metabolite, AUC_M and MTT_M, are not influenced by the changes in the vasculature. The AUC_M was unchanged with reversal of flow direction (Table 3). The MTT_M for retrograde flow was significantly shorter than that for prograde flow (Table 4; $P < 0.05$), and the partition ratio (influx/efflux) of benzoate exceeded that for hippurate. The data are consistent with the theoretical prediction for a perivenous distribution of benzoate conjugation activity (Table 1). This metabolic heterogeneity suggested by moment analysis reflects that there is zonation of the enzyme, benzoyl CoA ligase (Schwab et al., 2001). Moreover, due to the rapid transport of benzoate, transport would not affect the overall conjugation rate of benzoate since it is not the rate-determining step (Schwab et al., 2001).

The investigations on uptake corroborated with previous evidence on the lack of zonal transport of benzoate (Fig. 2), but the metabolic studies with zonal hepatocytes failed to provide the expected higher perivenous distribution of benzoate conjugation activity (Fig. 3). A lack of in vitro substantiation was also observed for the glutathione S-transferase (GST) activities towards 1-chloro-2,4-dinitrobenzene (CDNB) and ethacrynic acid, both in incubation studies and Western blotting of immunoreactive Ya and Yb2 GSTs with zonal rat hepatocytes (Tirona et al., 1999). The observations were explained by the cross contamination of the zonal hepatocytes by cells from other regions and the lack of a steep gradient for conjugation activity despite that the activities are indeed higher in the perivenous region. Indeed, the speculation was confirmed with use of PP and PV lysates for incubation studies and Western blotting when these provided a sharper enrichment and less cross contamination between PP and PV cells; the higher GST activity in PV cells became apparent (Tirona et al., 1999). Hence, the lack of metabolic zonation for glycine conjugation within zonal hepatocytes in the present study is not definitive of a lack of zonation in the intact organ. This is primarily due to a limitation of the method for the preparation of enriched cells.

The tubes-in-series model, though less quantitative as the Goresky approach in incorporating flow-heterogeneity, was nonetheless useful for the study of metabolic heterogeneity in the intact liver with the indicator dilution technique in progradely and retrogradely perfused livers. Although it is well known that the sinusoidal transit time is

heterogeneous (Pang et al., 1994), the predictions afforded by the tubes-in-series model on the ranking of transit times should be preserved. In addition to the tubes-in-series model, another model, the tanks-in-series model (Gray and Tam, 1987; Saville et al., 1992) exists and may be another useful representation, since the impulse function resulting from an injection was similar to that for the Goresky's model. However, the tanks-in-series- model is an empirical model, and the number of compartments (N) necessary to describe the data would vary according to the drug (Gray and Tam, 1987). It was found that N approached a value of 2 for red blood cells, albumin, and lidocaine (Gray and Tam, 1987; Saville et al., 1992), and a similar, tanks-in-series model with $N = 2$ was able to fit the data of estrone sulfate and estrone in the recirculating perfused rat liver preparation (Tan et al., 2001). In fact, our simulations based on the preliminary development of this model with two compartments (one for upstream and one for downstream) showed that exceedingly similar characteristics to the tubes-in-series model were obtained (see Fig. 7). The predictions on the changes of the AUC_M and MTT_M for the tanks-in-series model with permeability and flow direction (data not shown) were similar to that of the tubes-in-series model (Table 1). These models may be useful approaches and further developed as zonal model (Abu-Zahra and Pang, 2000) to encompass enzyme and transport heterogeneity for the description of zonal, drug metabolism.

References

Abu-Zahra TN and Pang KS (2000) Effect of zonal transport and metabolism on hepatic removal: enalapril hydrolysis in zonal, isolated rat hepatocytes in vitro and correlation with perfusion data. *Drug Metab Dispos*. **28**:807-813.

Ballinger LN, Cross SE, and Roberts MS (1995) Availability and mean transit times of phenol and its metabolites in the isolated perfused rat liver. Normal and retrograde studies using tracer concentrations of phenol. *J Pharm Pharmacol* **47**:949-996.

Bronikowski TA, Dawson CA, and Linehan JH (1987) On indicator dilution and perfusion heterogeneity: a stochastic model. *Math Biosci* **83**:199-225.

Chan KK, Bolger MB and Pang KS (1985) Statistical moment theory in chemical-kinetics. *Analytical Chemistry* **57**:2145-2151.

Chiba M, Poon K, Hollands J, and Pang KS (1994) Glycine conjugation of benzoic acid and its acinar localization in perfused rat liver. *J Pharmacol Exp Ther* **268**:409-416.

Cong D, Fong AK, Lee R and Pang KS (2001) Absorption of benzoic acid in segmental regions of the vascularly perfused rat small intestine preparation. *Drug Metab Dispos* **29**:1539-1547.

DeLannoy IAM and Pang KS (1987) Effect of diffusional barriers on drug and metabolite kinetics. *Drug Metab Dispos* **15**:51-58.

Gatley SJ and Sherratt HS (1977) The synthesis of hippurate from benzoate and glycine by rat liver mitochondria. Submitochondrial localization and kinetics. *Biochem J* **166**:39-47.

Gray MR and Tam YK (1987). The series-compartment model for hepatic elimination. *Drug Metab Dispos* **15**:27-31.

Goresky CA (1963) A linear method for determining liver sinusoidal and extravascular volumes. *Am J Physiol* **204**:626-640.

Lassen NA and Perl W (1979) Tracer Kinetic Methods in Medical Physiology. Raven Press, New York.

Lindros KO and Pentïlla KE (1985) Digitonin-collagenase perfusion for efficient separation of periportal or perivenous hepatocytes. *Biochem J* **228:**757-760.

Lowry OH, Rosenbrough NJ, Farr AL, and Randall RJ (1951) Protein measurement with the folin phenol reagent. *J Biol Chem* **193**:265-275.

Mellick GD and Roberts MS (1994) The disposition of aspirin and salicylic acid in the isolated perfused rat liver: the effect of normal and retrograde flow on availability and mean transit time. *J Pharm Pharmacol* **48**:738-743.

Mellick GD, Anissimov YG, Bracken AJ, and Roberts MS (1997) Metabolite mean transit times in the liver as predicted by various models of hepatic elimination. *J Pharmacokinet Biopharm* **25**:477-505.

Pang KS (1995) Modeling of metabolite disposition. In, *Advanced Methods of Pharmacokinetic and Pharmacodynamic System Analysis Volume II*, (ed. D.Z. D'Argenio), Plenum Press, New York, pp 3-26.

Pang KS and Terrell JA (1981) Retrograde perfusion to probe the heterogeneous distribution of hepatic drug metabolizing enzymes in rats. *J Pharmacol Exp Ther* **216**:339-346.

Pang KS, Cherry WF, Accaputo J, Schwab AJ, and Goresky CA (1988) Combined hepatic arterial-portal venous and hepatic arterial-hepatic venous perfusions to probe the abundance of drug metabolizing activities: Perihepatic venous *O*-deethylation activity for phenacetin and periportal sulfation activity for acetaminophen in the once-through rat liver preparation. *J Pharmacol Exp Ther* **247**:690-700.

Pang KS, Koster H, Halsema ICM, Scholtens E, Mulder GJ, and Stillwell RN (1983) Normal and retrograde perfusion to probe the zonal distribution of sulfation and glucuronidation activities of harmol in the perfused rat liver preparation. *J Pharmacol Exp Ther* **224**:647-653.

Pang KS, Xu N and Goresky CA (1991) D_2O as a substitute for ^3H_2O, as a reference indicator in liver multiple-indicator dilution studies. *Am J Physiol* **261**:G929-936.

Pang KS, Sherman IA, Schwab AJ, Geng W, Barker III F, Dlugosz JA, Cuerrier G, and Goresky CA (1994) Role of the hepatic artery in the metabolism of phenacetin and acetaminophen: An intravital microscopic and multiple indicator dilution study in perfused rat liver. *Hepatology* **20**:672-683.

Roberts M, Donaldson JD, and Rowland M (1988) Models of hepatic elimination: comparison of stochastic models to describe residence time distributions and to predict the influence of drug distribution, enzyme heterogeneity and systemic recycling on hepatic elimination. *J Pharmacokinet Biopharm* 16:41-83.

Rose CP, Goresky CA, and Bach GG (1977) The capillary and sarcolemmal barriers in the heart. An exploration of labeled water permeability. *Circ Res* **41**:515-533.

Sato H, Sugiyama Y, Miyauchi S, Sawada Y, Iga T, and Hanano M (1986) A simulation study on the effect of a uniform diffusional barrier across hepatocytes on drug metabolism by evenly or unevenly distributed uni-enzyme in the liver. *J Pharm Sci* **75**:3-8.

Saville BA, Gray MR and Tam YK (1992) Experimental studies of transient mass transfer and reaction in the liver: interpretation with a heterogeneous compartment model. *J Pharm Sci* **81**:265-271.

Schwab AJ (1984) Extension of the theory of the multiple-indicator dilution technique to metabolic systems with an arbitrary number of rate constants. *Math Biosci* **71**:57-79.

Schwab AJ and Pang KS (1999) The multiple indicator dilution method for the study of enzyme heterogeneity in liver: Theoretical basis. *Drug Metab Dispos* **27**:746-755.

Schwab AJ, Tao L, Yoshimura T, Simard A, Barker F and Pang KS (2001) Hepatic uptake and metabolism of benzoate: a multiple indicator dilution, perfused rat liver study. *Am J Physiol Gastrointest Liver Physiol* **280**:G1124-1136.

St-Pierre MV and Pang KS (1993a) Kinetics of sequential metabolism. I. Formation and metabolism of oxazepam from nordiazepam and temazepam in the perfused murine liver. *J Pharmacol Exp Ther* **265**:1429-1436

St-Pierre MV and Pang KS (1993b) Kinetics of sequential metabolism of metabolites. II. Formation and metabolism of nordiazpeam and oxazepam from diazepam in the perfused murine liver. *J Pharmacol Exp Ther* **265**:1437-1445.

St-Pierre MV, Lee PI, and Pang KS (1992) A comparative investigation of hepatic clearance models: predictions of metabolite formation and elimination. *J Pharmacokinet Biopharm* **20**:105-145.

St-Pierre MV, Schwab AJ, Goresky CA, Lee W-F, Pang KS (1989) The multiple indicator dilution technique for characterization of normal and retrograde once-through rat liver perfusions. *Hepatology* **9**:285-296.

Staricoff MA, Cohen RD, Monson JP (1995) Carrier-mediated lactate entry into isolated hepatocytes from fed and starved rats: zonal distribution and temperature. *Biosci Rep* **15**:99-109.

Tamai I, Sai Y, Ono A, Kido Y, Yabuuchi H, Tankanaga H, Satoh E, Ogihara T, Amano O, Izeki S, and Tsuji A (1999) Immunohistochemcial and functional characterization of pH-dependent intestinal absorption of weak organic acids by the monocarboxylic acid transporter MCT1. *J Pharm Pharmacol* **51**:1113-1121.

Tan E, Tirona RG, and Pang KS (1999) Lack of zonal uptake of estrone sulfate in enriched periportal and perivenous isolated rat hepatocytes. *Drug Metab Dispos* **27**:336-341.

Tan E, Lu T, and Pang KS (2001) Futile cycling of estrone sulfate and estrone in the recirculating, perfused rat liver. *J Pharmacol Exp Ther* **297**: 423-436.

Tirona RG and Pang KS (1999) Bimolecular glutathione conjugation of ethacrynic acid and efflux of the glutathione adduct by periportal and perivenous rat hepatocytes. *J Pharmacol Exp Ther* **290**:1230-1241.

Yoshimura T, Schwab AJ, Tao L, Barker F, and Pang KS (1998) Hepatic uptake of hippurate: A multiple indicator dilution, perfused rat liver study. *Am J Physiol* **274**:G10-G20.

Xu N, Chow A, Goresky CA, and Pang KS (1990) Effects of retrograde flow on measured blood volume, Disse space, intracellular water space and drug extraction in the perfused rat

liver: characterization by the multiple indicator dilution technique. *J Pharmacol Exp Ther* **254**: 914-925.

Appendix: Tubes-In-Series Model

Moments for a Metabolite when Formation Occurs in the Mitochondria. The partial differential equations describing the movement of tracers are as follows:

$$\frac{\partial C_1}{\partial t} + \frac{\partial C_1}{\partial \tau} = k_{31}\theta' C_3 - k_{13}C_1 + \frac{1}{Q}\delta(t)\delta(\tau) \quad \text{(A1)}$$

$$\frac{\partial C_2}{\partial t} + \frac{\partial C_2}{\partial \tau} = k_{52}\theta' C_5 - k_{25}C_2 \quad \text{(A2)}$$

$$\frac{\partial C_3}{\partial t} = \frac{k_{13}C_1}{\theta'} + k_{43}C_4 - (k_{31} + k_{34})C_3 \quad \text{(A3)}$$

$$\frac{\partial C_4}{\partial t} = k_{34}C_3 - (k_{43} + k_{45})C_4 \quad \text{(A4)}$$

$$\frac{\partial C_5}{\partial t} = \frac{k_{25}C_2}{\theta'} + k_{45}C_4 - k_{52}C_5 \quad \text{(A5)}$$

where C_1 and C_2 are dose-normalized tracer concentrations (fraction of dose per ml) of the parent drug and metabolite, respectively, in the expanded (sinusoidal + interstitial) plasma space, C_3, and C_5 are the corresponding dose-normalized concentrations of drug and metabolite in the cytosol of hepatocytes, C_4 is the dose-normalized concentration of drug in mitochondria, t is time, τ is a space variable representing the cumulative transit time of a reference indicator from the entrance point of the sinusoid (equal to the ratio of the cumulative expanded plasma space to sinusoidal flow), Q is the flow of perfusate fluid through the liver, and $\theta' = \theta/(1 + \gamma_{ref})$, where θ is the ratio of the accessible cellular water space to the sinusoidal volume and γ_{ref} is the volume ratio of extracellular space of the reference indicator to the sinusoidal volume.

Laplace transformation and elimination of the Laplace transforms of C_3, C_4, and C_5 yields the following system of ordinary differential equations in τ:

$$\frac{d\tilde{C}_1}{d\tau} = -\left[s + \frac{k_{34}k_{43} - (s + k_{34})(s + k_{43} + k_{45})}{k_{34}k_{43} - (s + k_{31} + k_{34})(s + k_{43} + k_{45})} k_{13} \right] \tilde{C}_1 + \delta(\tau) \quad \text{(A6)}$$

JPET Fast Forward. Published on January 21, 2003 as DOI: 10.1124/jpet.102.044024
This article has not been copyedited and formatted. The final version may differ from this version.

$$\frac{d\tilde{C}_2}{d\tau} = -\frac{k_{13}k_{34}k_{45}k_{52}}{\left[s+k_{52}\right]\left[k_{34}k_{43}-(s+k_{31}+k_{34})(s+k_{43}+k_{45})\right]}\tilde{C}_1 - s\left(1+\frac{k_{25}}{s+k_{52}}\right)\tilde{C}_2 \qquad \text{(A7)}$$

where $\tilde{C}_1(s)$ and $\tilde{C}_2(s)$ are the Laplace transforms of C_1 and C_2, respectively, and s is the Laplace variable. The solutions are

$$\tilde{C}_1(s) = \frac{1}{Q}e^{-\lambda_1(s)\tau} \qquad \text{(A8)}$$

$$\tilde{C}_2(s) = \frac{k_{13}k_{34}k_{45}k_{52}\left[e^{-\lambda_1(s)\tau} - e^{-\lambda_2(s)\tau}\right]}{Q\left\{k_{13}(s+k_{52})\left[k_{34}k_{43}-(s+k_{34})(s+k_{43}+k_{45})\right] - k_{25}s\left[k_{34}k_{43}-(s+k_{31}+k_{34})(s+k_{43}+k_{45})\right]\right\}} \qquad \text{(A9)}$$

where the exponential coefficients, λ_1 and λ_2, are

$$\lambda_1(s) = s + \frac{k_{34}k_{43}-(s+k_{34})(s+k_{43}+k_{45})}{k_{34}k_{43}-(s+k_{31}+k_{34})(s+k_{43}+k_{45})}k_{13} \qquad \text{(A10)}$$

$$\lambda_2(s) = s\left(1+\frac{k_{25}}{s+k_{52}}\right) \qquad \text{(A11)}$$

The area under the curve (AUC) or zeroth moment for drug is obtained from the following equation:

$$\begin{aligned}\text{AUC} &= \int_0^\infty C_1(t)dt \\ &= \lim_{s\to 0}\tilde{C}_1(s)\end{aligned} \qquad \text{(A12)}$$

The recovery (survival fraction, or availability, F) is obtained as the product of AUC and the plasma flow rate, Q.

$$F = AUC\ Q \tag{A13}$$

The mean transit time (MTT) or first moment is obtained from the following equation:

$$\begin{aligned} MTT &= \frac{1}{AUC}\int_0^\infty tC_1(t)dt \\ &= \frac{-1}{AUC}\lim_{s\to 0}\frac{\partial \tilde{C}_1(s)}{\partial s} \end{aligned} \tag{A14}$$

Substitution of eq. A6 into Eqs. A12 and 14 yields the following analytical expressions for the zeroth (AUC) and first (MTT) moments of the parent drug:

$$AUC = \frac{1}{Q}e^{-\frac{k_{45}k_{34}k_{13}}{k_{45}k_{34}+k_{45}k_{31}+k_{43}k_{31}}\tau} \tag{A15}$$

$$MTT = \left[1+\frac{k_{13}k_{31}\left[k_{34}k_{43}+(k_{43}+k_{45})^2\right]}{\left(k_{31}k_{43}+k_{31}k_{45}+k_{34}k_{45}\right)^2}\right]\tau \tag{A16}$$

Equations A15 and A16 are equivalent to those presented previously (Rose et al., 1977).

The moments for the preformed metabolite are:

$$AUC_{PM} = 1/Q \tag{A17}$$

$$MTT_{PM} = \left(1+\frac{k_{25}}{k_{52}}\right)\tau \tag{A18}$$

For the formed metabolite, the following analytical expressions are obtained similarly from eq. A9:

$$AUC_M = \frac{1}{Q}\left(1-e^{-\frac{k_{13}k_{34}k_{45}}{k_{31}k_{43}+k_{31}k_{45}+k_{34}k_{45}}\tau}\right) \tag{A19}$$

JPET Fast Forward. Published on January 21, 2003 as DOI: 10.1124/jpet.102.044024
This article has not been copyedited and formatted. The final version may differ from this version.

$$MTT_M = \frac{k_{13}\left(k_{34}k_{45} + k_{34}k_{52} + k_{43}k_{52} + k_{45}k_{52}\right) - k_{25}\left(k_{31}k_{43} + k_{31}k_{45} + k_{34}k_{45}\right)}{k_{13}k_{34}k_{45}k_{52}}$$
$$+\left\{\frac{1+\frac{k_{25}}{k_{52}}}{1-e^{-\frac{k_{13}k_{34}k_{45}}{k_{31}k_{43}+k_{31}k_{45}+k_{34}k_{45}}\tau}} + \frac{1+\frac{k_{13}k_{31}\left[k_{34}k_{43}+(k_{43}+k_{45})^2\right]}{\left(k_{31}k_{43}+k_{31}k_{45}+k_{34}k_{45}\right)^2}}{1-e^{\frac{k_{13}k_{34}k_{45}}{k_{31}k_{43}+k_{31}k_{45}+k_{34}k_{45}}}}\right\}\tau \qquad \text{(A20)}$$

Figure Legends

Fig. 1. Theoretical models of metabolism. Model A, metabolism in the cytosol according to Schwab and Pang (1999). k_{13} and k_{31} are coefficients for influx of tracer precursor into, and efflux from, parenchymal cells; k_{24} and k_{42} are the corresponding coefficients for the metabolite; k_{34} is the coefficient for enzymic conversion of parent to metabolite; k_{30} is that for sequestration (removal) of the parent drug (other than formation of the metabolite), and k_{40} is that for sequestration of the metabolite. Model B, metabolite formation in a deep compartment (compartment 4), k_{13} and k_{31} as above, k_{25} and k_{52} are the coefficients for influx and efflux for the metabolite; k_{45} is the coefficient for glycine conjugation of benzoate; k_{30} (coefficient for additional sequestration of benzoate) and k_{50} (coefficient for sequestration of the metabolite) are set to zero.

Fig. 2. Uptake of benzoate by periportal (n = 3), homogeneous (n = 4), and perivenous (n = 3) isolated rat hepatocytes for 1 and 400 μM benzoate. Data were mean ± SD.

Fig. 3. Lack of zonal difference in metabolism of benzoate (1 μM) by PP and PV hepatocytes (1.6 to 1.7 x 10^6 cells/ml) in formation of hippurate. The disappearance of benzoate from PP (▲) and PV (Δ) cells was accounted for by formation of hippurate in PP (▼) and PV (∇) cells. Data were mean ± SD of four preparations each.

Fig. 4. Outflow profiles of the preformed metabolite, [^{3}H]hippurate, and the noneliminated references, pursuant to first MID injection. The representative single pass study was conducted at 17 μM of the precursor, benzoate. Data are presented as fractions of dose recovered per ml of perfusate and are plotted in linear (top) and semilogarithmic (bottom) formats. The continuous line in the bottom panel represents the fitted outflow profile.

Fig. 5. Outflow profiles of [^{14}C]benzoate, its metabolite, [^{14}C]hippurate, and the noneliminated references. The representative single pass study was conducted at 17

μM benzoate. Data are presented as fractions of dose recovered per ml of perfusate and are plotted in linear (top) and semilogarithmic (bottom) formats. The continuous and broken lines in the bottom panel represent the fitted outflow profiles for parent drug and metabolite, respectively.

Fig. 6. Distention of the vascular spaces during retrograde perfusion (hatched bar) over prograde perfusion (dotted bar); * significantly different, with $P < 0.05$.

Fig. 7. Effect of the heterogeneity factor (r) on the PP:PV ratio of MTT_M with the tubes-in-series or Tube model. The fitted parameters k_{13}, k_{31}, k_{25}, k_{52}, k_{34}, and k_{45} (Table 5) were used in the simulation. The value of $r = 1$ indicates exclusive PP metabolic zonation (enzyme present in first half of liver); the value of $r = -1$ represents exclusive PV metabolic zonation (enzyme present in second half of liver); $r = 0$ indicates evenly distributed metabolic activity. Further simulation was performed with the parameters, based on a two compartment tanks-in-series model. Similar trends were obtained.

TABLE 1

Expected behavior of moments (zeroth moment or AUC_M and first moment or MTT_M) of the generated metabolite with prograde/retrograde perfusion ($k_{30} = k_{50} = 0$, Fig. 2) for which the mitochondrial compartment is present for metabolite formation (see Fig. 1B).

		Enzyme Distribution	
Parameter	**Condition**	Periportal	Perivenous
AUC_M	$(k_{13}/k_{31})(1 + k_{34}/k_{43}) < k_{25}/k_{52}$	Prograde = Retrograde	Prograde = Retrograde
	$(k_{13}/k_{31})(1 + k_{34}/k_{43}) > k_{25}/k_{52}$	Prograde = Retrograde	Prograde = Retrograde
MTT_M	$(k_{13}/k_{31})(1 + k_{34}/k_{43}) < k_{25}/k_{52}$	Prograde < Retrograde	Prograde > Retrograde
	$(k_{13}/k_{31})(1 + k_{34}/k_{43}) > k_{25}/k_{52}$	Prograde > Retrograde	Prograde < Retrograde

TABLE 2

Steady state data for retrograde perfusion of benzoate in the present studies were compared to those for prograde perfusion at similar concentrations of benzoate (data from Schwab et al., 2001)[a]

	Rat (g)	Liver (g)	Flow (ml/sec/g)	Hematocrit	Parameters for Benzoate	
					C_{In} (μM)	E[b]
Retrograde (*n* = 8)	296 ± 9	11.1 ±2.2	0.020 ±0.005	0.14 ±0.004	15 to 18	0.60 ±0.09
Prograde (*n* = 7)	325 ±29	11.8 ±1.5	0.017 ±0.002	0.16* ±0.01	10 to 179	0.59 ±0.19

[a] data were mean±S.D.

[b] steady state extraction ratio

*different from retrograde, $P < 0.05$

TABLE 3

Recoveries of noneliminated reference indicators and labeled hippurate and benzoate after injection of MID doses of [^{3}H]hippurate and [^{14}C]benzoate during retrograde perfusion were compared to those published by Schwab et al. (2001) for retrograde perfusion[a]

	Tracer Recoveries							% (HA+BA)	
	^{51}Cr-labeled RBC	^{125}I-labeled Albumin	Labeled Sucrose	$^{2}H_2O$	Hippurate (HA)	Benzoate (BA)	Hippurate + Benzoate	HA[b]	BA[c]
Hippurate Injection									
Retrograde (n = 8)	0.97±0.13	0.91±0.08	1.11±0.25	0.98±0.04	0.96±0.06				
Prograde (n = 7)	1.04±0.11	1.02±0.13	0.99±0.10	1.01±0.12	1.03±0.08				
Benzoate Injection									
Retrograde (n = 8)	1.03 ± 0.09	0.92±0.07	1.29±0.19		0.49±0.09	0.45±0.05	1.94±0.09	52±5	48±5
Prograde (n = 7)	1.09±0.10	1.02±0.13	0.95±0.21*		0.42±0.12	0.49±0.16	0.90±0.21	49±11	51±11

[a]data were mean±S.D

[b] ratio of recoveries: HA/(HA+BA)

[c] ratio of recoveries: BA/(HA+BA)

* $P < 0.05$, prograde vs. retrograde

TABLE 4

Transit times of outflow profiles for the noneliminated reference indicators and preformed hippurate and benzoate during retrograde perfusion were compared to those of Schwab et al. (2001) for prograde perfusion of benzoate.

Tracer Injected	**Catheter-corrected MTT (sec)**					
	^{51}Cr-labeled RBC	^{125}I-labeled Albumin	Labeled Sucrose	$^{2}H_2O$	Hippurate	Benzoate
First Injection: Hippurate						
Retrograde (*n* = 8)	18.0±2.4	23.6±2.9	32.5±4.2	55±9	29.5±4.1	
Prograde (*n* = 7)	11.0±2.5*	17.0±3.1*	20.5±3*	59±8	29.3±3.1	
Second Injection: Benzoate						
Retrograde (*n* = 8)	14.5±2.7†	20.5±3.7	21.3±4.8†		67.2±7.3	22.4±2.4
Prograde (*n* = 7)	10.8±2.9*	16.7±3.6	20.5±4.9		100 ±32*	26.6±11

[a]data were mean±S.D of fractions of complete recovery (AUC/perfusate flow rate)

* $P < 0.05$, vs. retrograde data for first or second injection

† $P < 0.05$, vs. first injection retrograde data

TABLE 5

Fitted parameters obtained for preformed hippurate and benzoate (see Figure 1 for definition of terms) from MID studies with retrograde perfusion versus those obtained from Schwab et al. (2001) for prograde perfusion[a]

	Parameters for Benzoate						Parameters for Hippurate			Other parameters	
	$P_{13}S$ (ml/sec/g)	k_{13} (sec^{-1})	k_{31} (sec^{-1})	k_{34} (sec^{-1})	k_{43} (sec^{-1})	k_{45} (sec^{-1})	$P_{25}S$ (ml/sec/g)	k_{25} (sec^{-1})	k_{52} (sec^{-1})	t_0 for 1st injection (sec)	t_0 for 2nd injection (sec)
Retrograde (n = 8)	1.58 ±0.61	0.30 ±0.11	0.48 ±0.24	0.12 ±0.02	0.0055 ±0.0014	0.041 ±0.01	0.062 ±0.029	0.031 ±0.012	0.13 ±0.07	2.6 ±1.2	3.5 ±1.0
Prograde[a] (n = 7)	0.90* ±0.07	0.25 ±0.04	0.16* ±0.05	0.07* ±0.02	0.0062 ±0.0020	0.026* ±0.014	0.056 ±0.023	0.082* ±0.029	0.090 ±0.041	4.3* ±0.8	2.6 ±1.5

[a]For BA, k_{13}/ $k_{31}$was 1.68 for prograde and 0.7 for retrograde; for HA; k_{25}/ $k_{52}$was 0.81 for prograde and 0.26 for retrograde. Values for prograde and retrograde were statistically different.

JPET Fast Forward. Published on January 21, 2003 as DOI: 10.1124/jpet.102.044024
This article has not been copyedited and formatted. The final version may differ from this version.

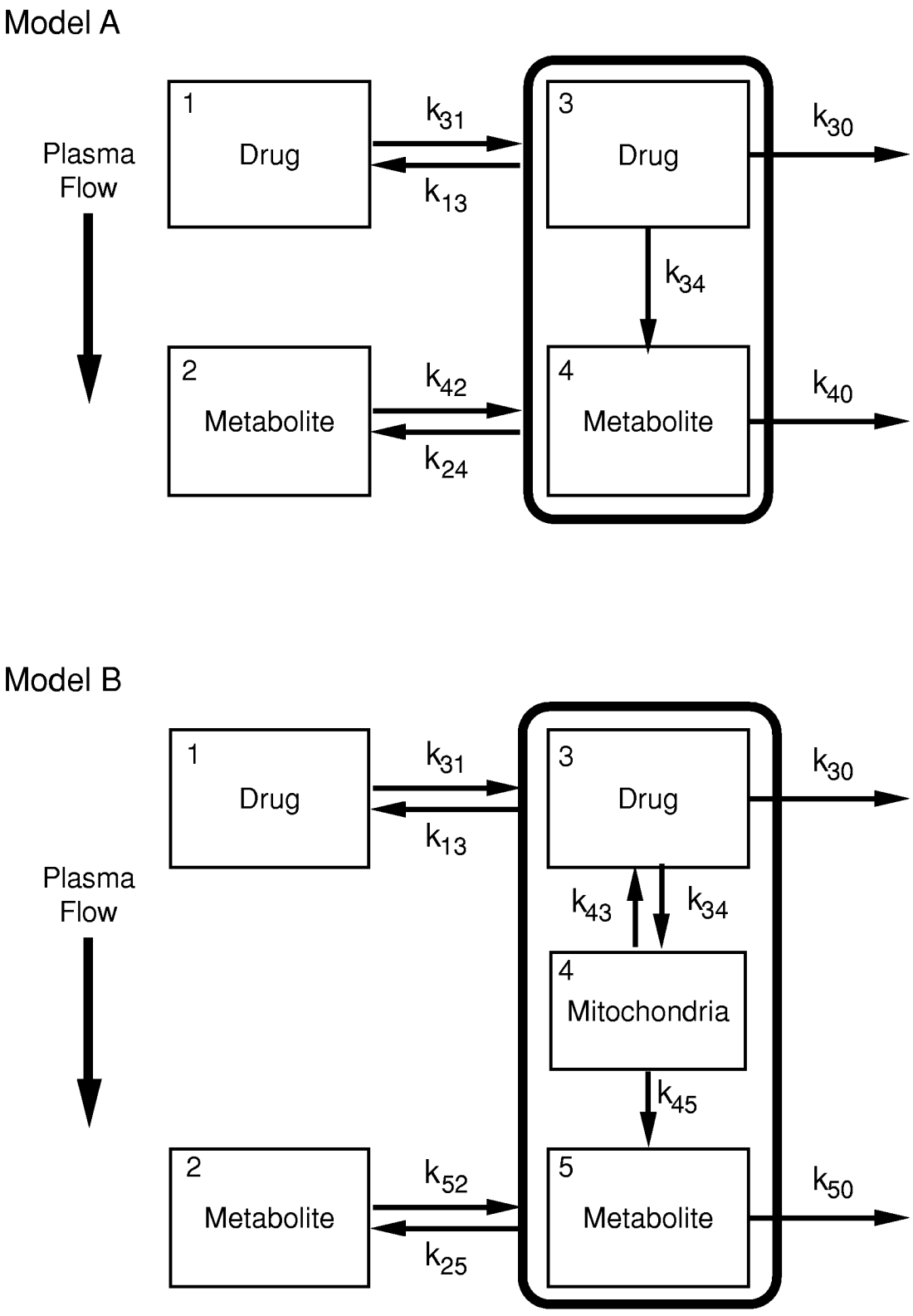

Figure 1

JPET Fast Forward. Published on January 21, 2003 as DOI: 10.1124/jpet.102.044024
This article has not been copyedited and formatted. The final version may differ from this version.

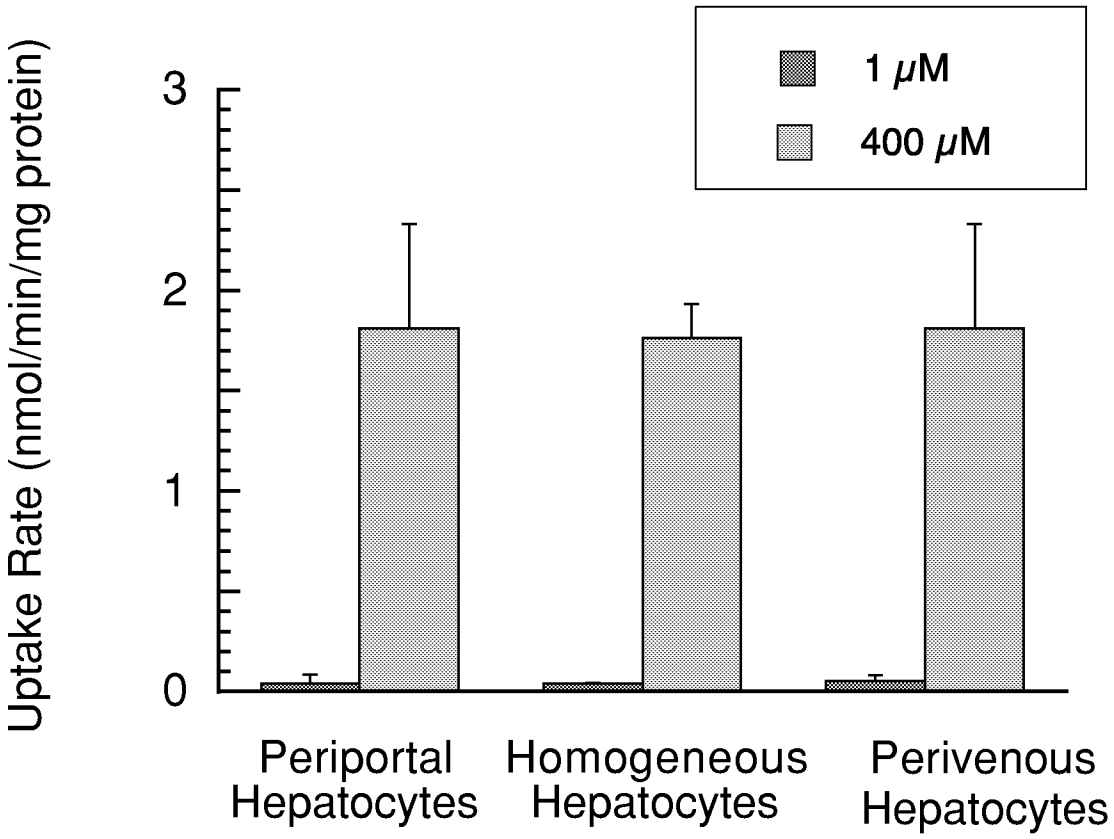

Figure 2

JPET Fast Forward. Published on January 21, 2003 as DOI: 10.1124/jpet.102.044024
This article has not been copyedited and formatted. The final version may differ from this version.

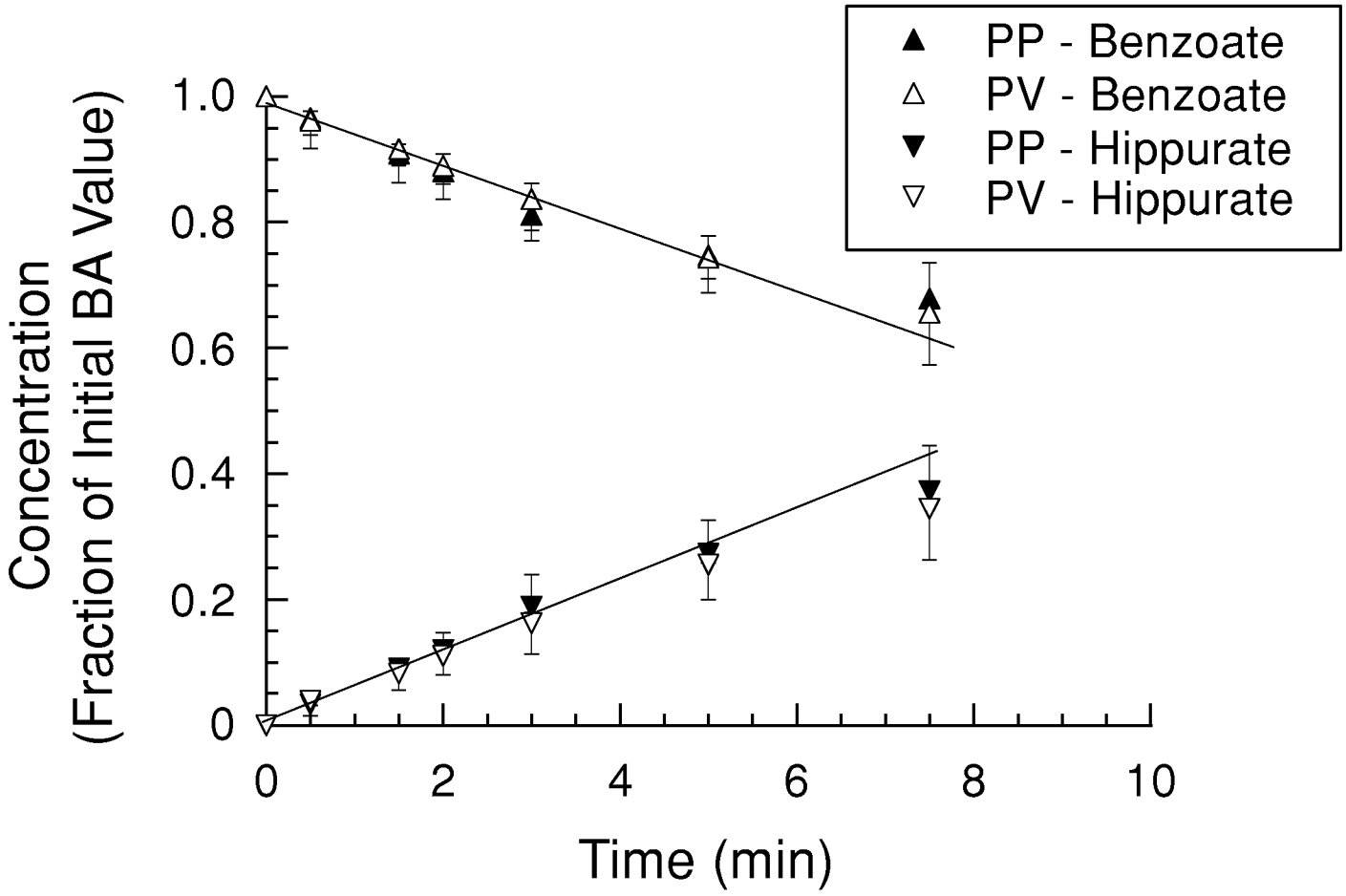

Figure 3

JPET Fast Forward. Published on January 21, 2003 as DOI: 10.1124/jpet.102.044024
This article has not been copyedited and formatted. The final version may differ from this version.

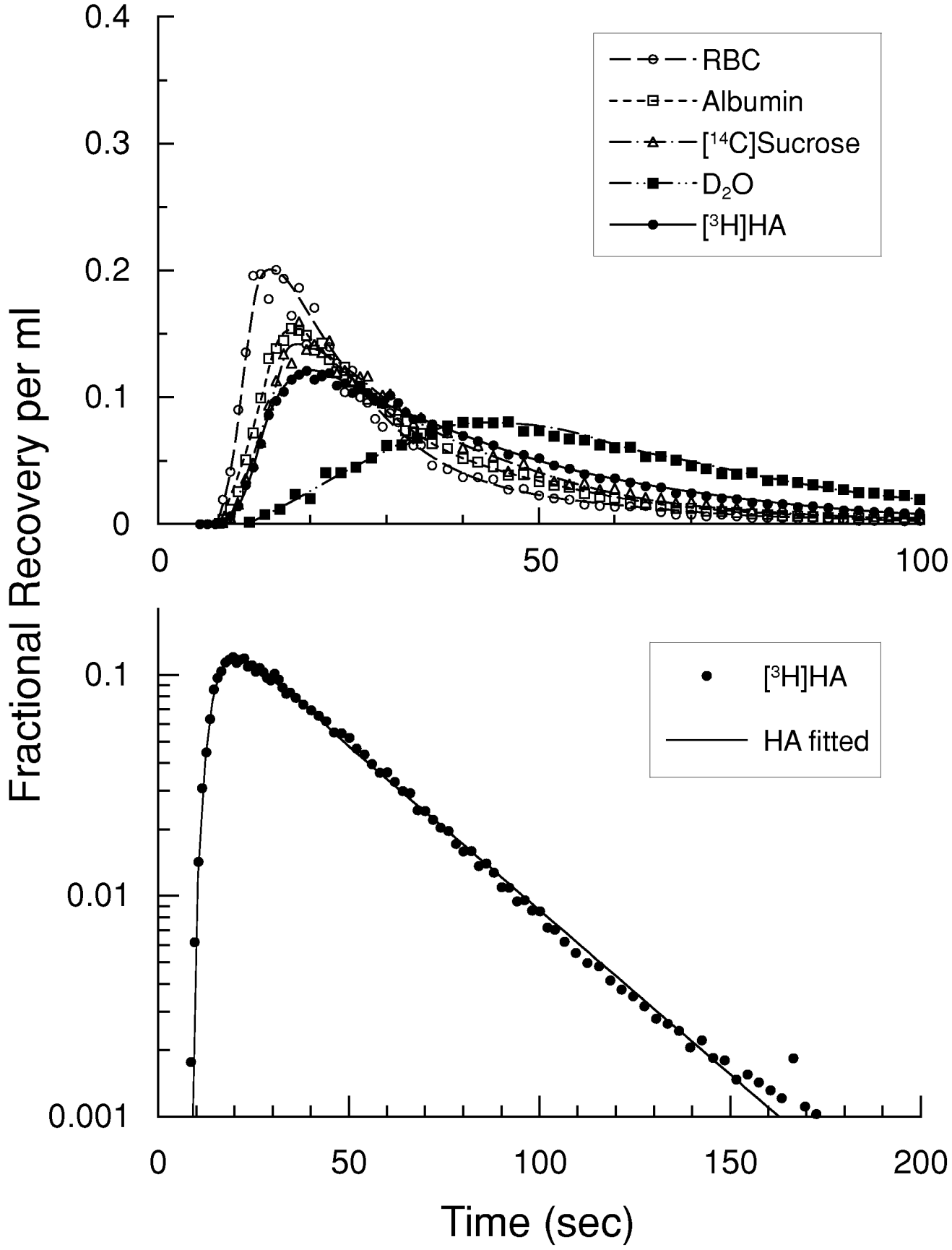

Figure 4

JPET Fast Forward. Published on January 21, 2003 as DOI: 10.1124/jpet.102.044024
This article has not been copyedited and formatted. The final version may differ from this version.

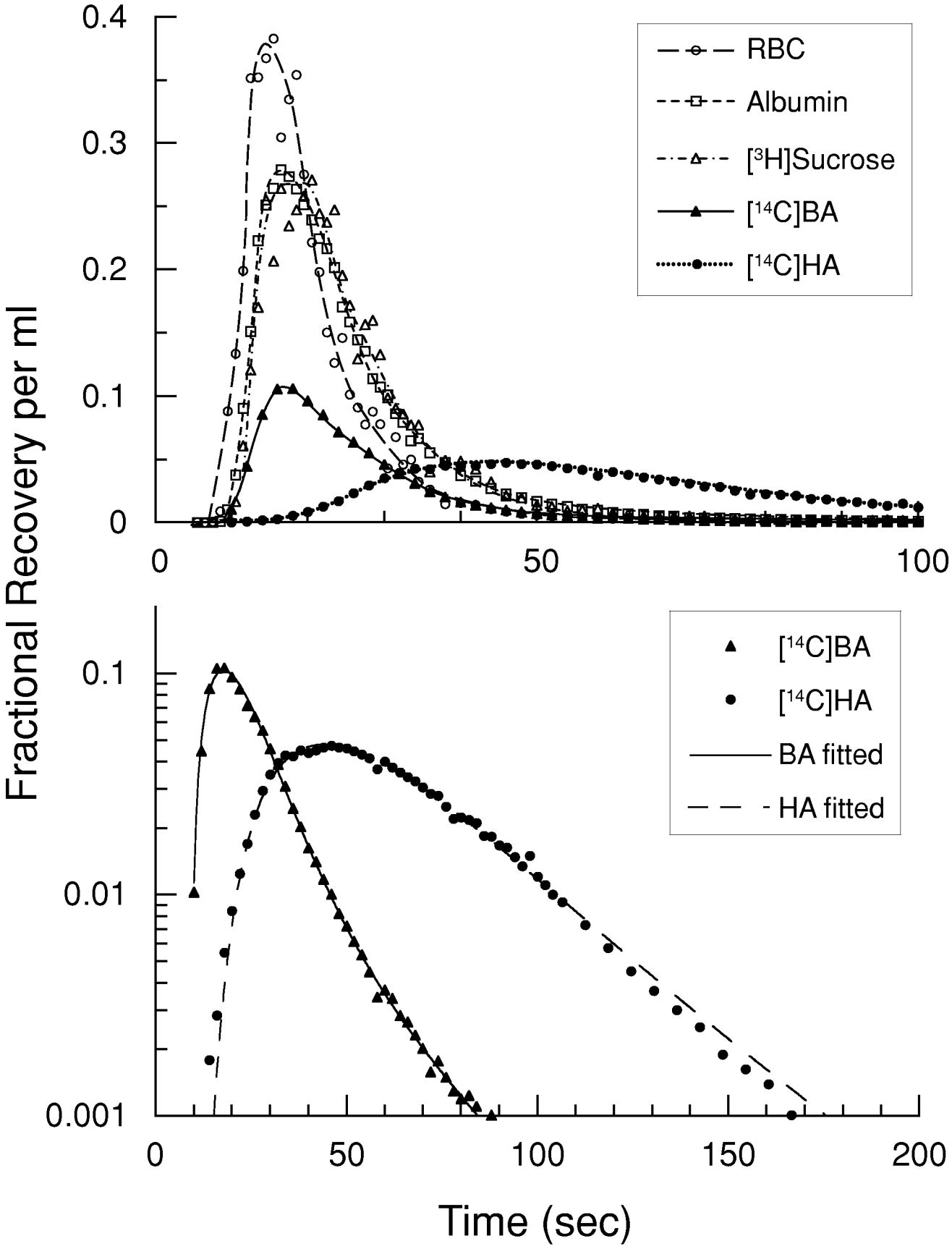

Figure 5

JPET Fast Forward. Published on January 21, 2003 as DOI: 10.1124/jpet.102.044024
This article has not been copyedited and formatted. The final version may differ from this version.

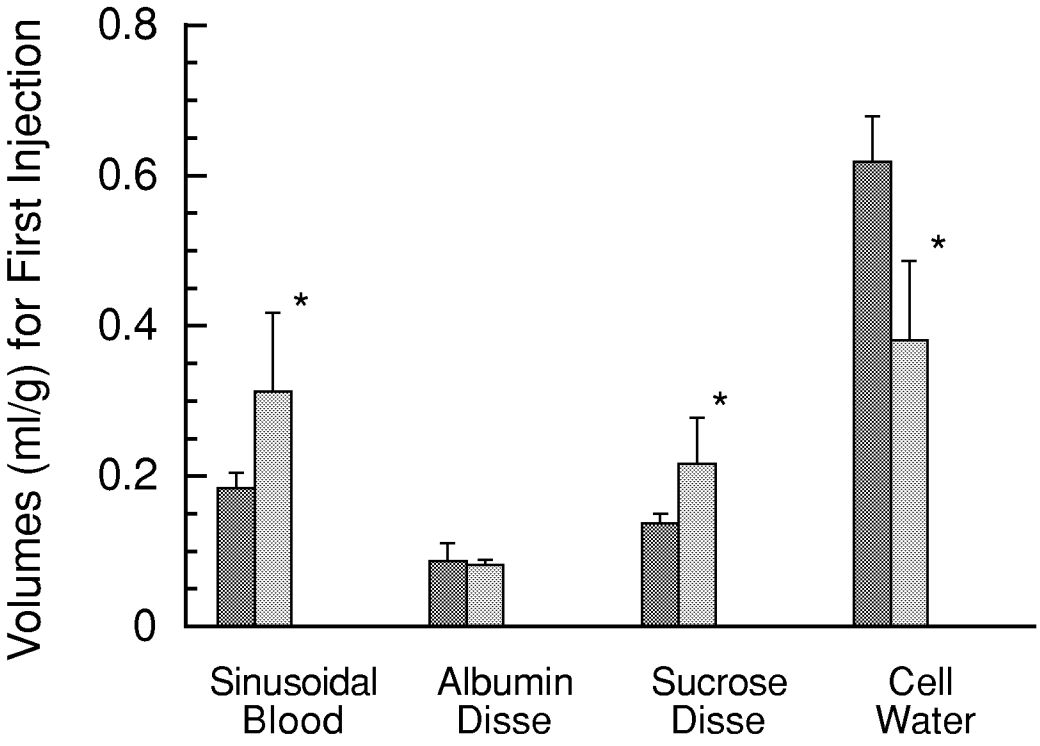

Figure 6

JPET Fast Forward. Published on January 21, 2003 as DOI: 10.1124/jpet.102.044024
This article has not been copyedited and formatted. The final version may differ from this version.

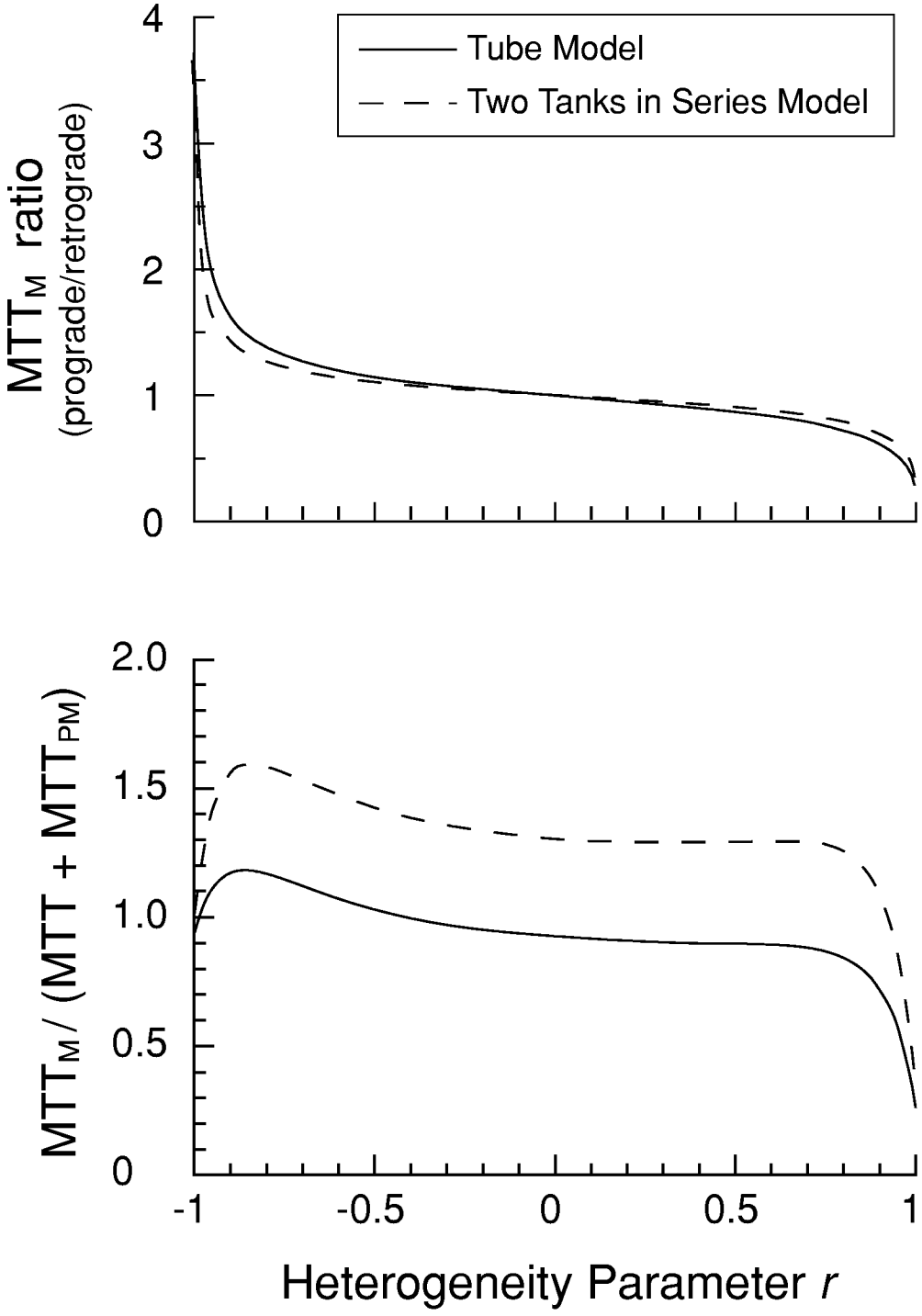

Figure 7